Selective excitation through multiphonon emission of ZnCdTe quantum dots embedded in Zn-rich ZnCdTe quantum wells

Yannick Viale, Pierre Gilliot,* Olivier Crégut, Jean-Pierre Likforman, Mathieu Gallart, and Bernd Hönerlage
Institut de Physique et Chimie des Matériaux de Strasbourg-GONLO, UMR7504 CNRS-Université Louis Pasteur (Strasbourg I), 23 rue du Læss, B.P. 43, F-67034 Strasbourg CEDEX 2, France

Kuntheak Kheng and Henri Mariette
Equipe Nanophysique et Semiconducteurs, Laboratoire de Spectrométrie Physique, Université Joseph Fourier, Département de Recherche Fondamentale sur la Matière Condensée/SP2M, CEA-Grenoble, 17 Avenue des Martyrs, F-38054 Grenoble CEDEX 9, France
(Received 21 August 2003; revised manuscript received 5 December 2003; published 19 March 2004)

We study the energy relaxation of electron-hole pairs in ZnCdTe quantum wells, which is followed by a trapping in self-organized CdTe/ZnTe islands. An optical-phonon emission cascade is observed, giving rise to a selective population of the Cd-rich islands. Using photoluminescence excitation spectroscopy, we determine the energy of the phonons involved in the process. We study also the evolution of the quantum efficiency of the phonon emission process as a function of the photon energy, the number of emitted phonons, and temperature. Moreover, we evidence coupled exciton-phonon states in the quantum dots which explain the trapping of the electron-hole pairs and their recombination.

DOI: 10.1103/PhysRevB.69.115324 PACS number(s): 78.67.Hc, 78.55.Et, 71.38.Ht

I. INTRODUCTION

Semiconductor technology makes it possible to grow quantum dots (QD) structures in which carrier confinement is achieved in all three spatial dimensions. With regard to bulk, in such QD's, the relaxation processes of electron-hole pairs undergo intrinsic modifications as a consequence of the discrete density of states of these quasi-zero-dimensional structures, as well as extrinsic modifications due the interactions with the supporting matrix or the substrate. Although the relaxation of electron-hole pairs in QD's has been intensively studied,[1–7] only few experiments have been performed on CdTe/ZnTe structures.[8] In this system, high-order optical-phonon mediated relaxation, similar to phenomena observed in GaAs QD's,[9] has been reported recently.[10]

In this paper, we present a study of the optical-phonon emission cascades in Zn-rich ZnCdTe quantum wells (QW's) followed by a trapping of electron-hole pairs in Cd-rich ZnCdTe QD's. In the QD's, the electron-hole pairs recombine radiatively, giving rise to the observed photoluminescence (PL). From the analysis of photoluminescence excitation (PLE) intensities and in the framework of a simple model, we determine the quantum efficiency of longitudinal optical-phonon emission in the QW's as well as its energy and temperature dependence.

II. EXPERIMENTAL DETAILS

A. Sample description

Our sample is grown by atomic-layer epitaxy on a (0 0 1)-ZnTe substrate, as described with more details in Ref. 11. It contains ten CdTe QD layers separated by 10-nm-thick ZnTe layers. Each QD layer has been obtained by deposing 6.5 monolayers of CdTe on the ZnTe barrier layer. The analysis of transmission electron microscopy (TEM) images[12] reveals that the QD's actually consist of Cd-rich ZnCdTe islands confined along the growth direction by pure ZnTe barriers and confined laterally by Zn-rich ZnCdTe. The actual structure can be viewed as Cd-rich ZnCdTe QD's embedded in Zn-rich ZnCdTe quantum wells. The QD diameter is about 20 nm and its height 4 nm. Their density is 2×10^{10} cm^{-2}.

B. Experimental setup

In the PLE spectroscopy measurements described here, the emission of a xenon lamp is spectrally filtered by a monochromator to obtain an excitation bandwidth of 4 meV [full width at half maximum (FWHM)] and a photon energy that can be tuned between 1.9 and 2.5 eV. The filtered light excites the sample whose temperature is kept fixed between 4 and 100 K in a cold-finger cryostat. The PL is dispersed in a spectrometer and detected by a cooled charge-coupled device camera. The overall spectral resolution of the PL measurement is about 1 meV.

III. EXPERIMENTAL RESULTS

A. Absorption and emission spectra for barrier excitation

Figure 1 shows the luminescence and absorption spectra of our sample. The unavoidable dispersion of the QD parameters (size, shape, composition, etc.) leads to a broad distribution of excitonic levels of the QD's, resulting in an inhomogeneously broadened optical line (band of sharp excitonic lines). The PL spectrum in Fig. 1 is obtained when exciting with photon energies higher than that of the barriers. The electron-hole pairs, which are photocreated in the barriers, are trapped in the QD's after energy relaxation and their recombination in the QD's gives rise to the luminescence band (centered at $\hbar\omega_{\mathrm{PL}}^{M}=1.971$ eV at 4 K). The luminescence spectrum is unstructured and has a Gaussian shape

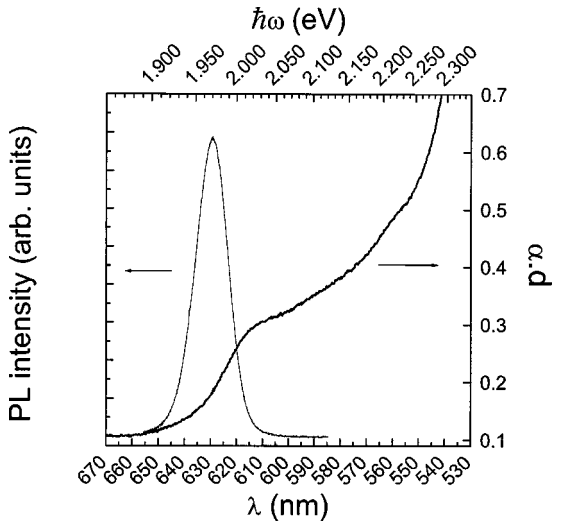

FIG. 1. Photoluminescence and absorption spectra of the sample at 4 K. The PL is excited at 2.480 eV, i.e., above the band gap of the ZnTe barrier. The spectrum shows the inhomogeneously broadened exciton band of the quantum dots. The linear absorption spectrum shows a weak maximum associated to the maximum of excitonic density of states inside the dots.

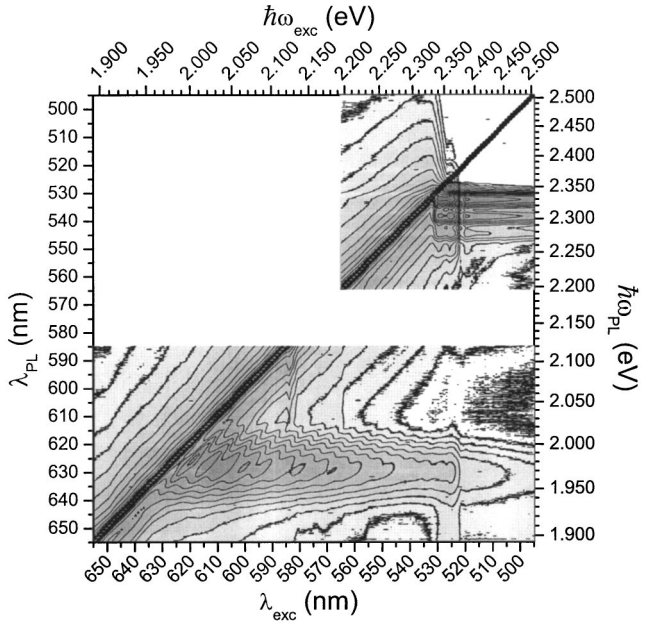

FIG. 2. Sample emission at 5.7 K plotted as a function of the exciting photon energy $\hbar\omega_{\mathrm{exc}}$ (X axis) and of the emission photon energy $\hbar\omega_{\mathrm{PL}}$ (Y axis). The intensity is plotted using a logarithmic scale with six contour lines and gray values for a decade. Along the diagonal is aligned the Rayleigh scattering of the exciting light.

with an inhomogeneous linewidth of 50 meV (FWHM). The absorption spectrum shows a local structure superimposed onto a continuous increase of absorption ranging from the spectral position of the QD luminescence to the ZnTe barrier absorption edge. This maximum is attributed to the discrete QD states because absorption due to delocalized states in the QW layer is expected to be at larger photon energies. When subtracting the monotonously increasing background from the absorption, we obtain an unstructured absorption band centered at 2.105 eV with a half width (FWHM) of 50 meV. We suppose that absorption and luminescence bands are involving the same states of the QD's. The observed Stokes shift $\Delta=\hbar\omega_A^M-\hbar\omega_{\mathrm{PL}}^M=44$ meV of the luminescence with respect to the absorption gives an estimate for the strength of the electron-phonon interaction. From the analysis of HR-TEM images, the cadmium concentration of the $\mathrm{Cd}_x\mathrm{Zn}_{1-x}\mathrm{Te}$ QD's can be estimated to be $x=0.8$. They are embedded in a QW layer which has a thickness less than 6.5 monolayers and a lower cadmium concentration (below 0.4).

B. Photoluminescence excitation spectra

For an excitation close to or below the ZnTe barrier gap, the emission spectra of the sample at 5.7 K are shown in Fig. 2 where the photoluminescence intensity $I(\hbar\omega_{\mathrm{exc}},\hbar\omega_{\mathrm{PL}})$ is plotted as a function of both the excitation energy $\hbar\omega_{\mathrm{exc}}$ and the emission photon energy $\hbar\omega_{\mathrm{PL}}$. The gray scale of the shaded areas is proportional to the logarithm of PL intensity. PL and PLE spectra can be extracted from Fig. 2 as cross sections along the Y axis and X axis, respectively.

Figure 3 shows the PL spectra at 5.7 K when exciting the sample at 2.363 and 2.390 eV, i.e., within the ZnTe barriers and close to the exciton resonance of bulk ZnTe situated at 2.375 eV. A strong bound exciton luminescence line shows up at 2.328 eV, followed by two well defined LO phonon replicas at 2.302 and 2.277 eV. The energy separation of 26 meV is in good agreement with the energy of longitudinal-optical phonons in bulk ZnTe of 25.8 meV.[13] These strong emission lines have fixed spectral positions when the photon energy of the excitation is changed, indicating that the excited electron-hole pairs have efficiently thermalized in the barriers by emission of phonons and mutual scattering. This result is in agreement with the fact that only a weak QD emission is observed around 1.965 eV (Fig. 2): only few of the electron-hole pairs photocreated in the ZnTe barriers are being trapped into CdTe dots because the vast majority of pairs recombines directly within the ZnTe barriers without

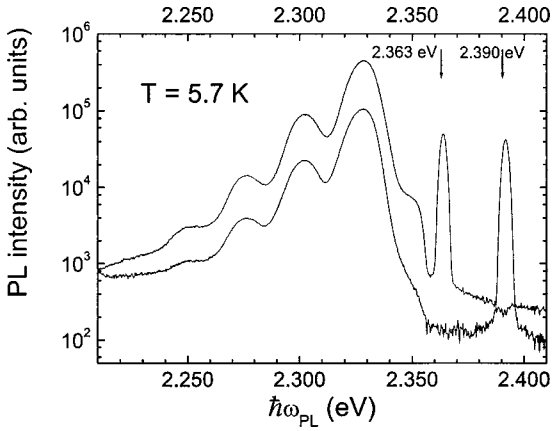

FIG. 3. Photoluminescence spectra at 5.7 K when exciting the ZnTe barriers at 2.363 and 2.390 eV, close to the ZnTe exciton resonance. This corresponds to cross sections of Fig. 2 parallel to the Y axis.

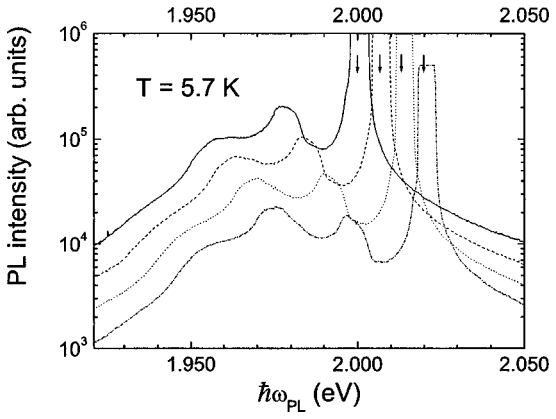

FIG. 4. Photoluminescence spectra at 5.7 K when exciting the QW states far below the photon energy of the ZnTe barriers. This corresponds to cross sections of Fig. 2 parallel to the *Y* axis.

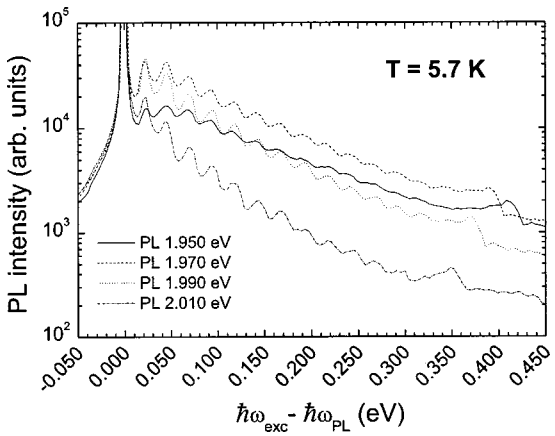

FIG. 5. Photoluminescence excitation spectra determined from Fig. 2 as function of the difference of the photon energy of the exciting light $\hbar\omega_{\mathrm{exc}}$ and that of the photoluminescence $\hbar\omega_{\mathrm{PL}}$. This corresponds to cross sections of Fig. 2 parallel to the *X* axis.

further relaxation. It is important to notice that no emission is observed in between the phonon replica of the ZnTe bound exciton and the QD luminescence.

The situation becomes different when exciting at lower photon energies. Figure 4 shows the PL spectrum when exciting the sample farther below the ZnTe barrier gap. Beside the Rayleigh scattered light of the excitation, the photoluminescence intensity of the QD's is now stronger. The electron-hole pairs are now photocreated within the CdZnTe layers and they are more efficiently trapped in the QD's. The QD PL intensity distribution, however, has no longer a Gaussian shape as in Fig. 1 but shows three secondary maxima. These are separated by about 24 meV from each other, and, as will be discussed in the following, are due to emission of several longitudinal optical phonons before the electron-hole pairs recombine radiatively within the QD's.

The spectral positions of the PL intensity maxima now change when the photon energy of the excitation is changed. The energy separation between excitation and emission maxima corresponds to an integer number of optical-phonon energies $\hbar\omega_{\mathrm{LO}}$. Only QD's which have exciton levels separated from the excitation energy by an integer number of optical-phonon energies are selectively populated. A Dirac comb with a step given by the phonon energy $\hbar\omega_{\mathrm{LO}}$ and a spectral shift determined by the excitation photon energy is thus imprinted in the broad inhomogeneous emission line of the dot. This shows that the main mechanism for the exciton relaxation from the barriers into the dots is the emission of LO phonons.

Figure 5 shows PLE spectra extracted from the data of Fig. 2. The emission intensity is plotted as function of $\Delta E = \hbar\omega_{\mathrm{exc}} - \hbar\omega_{\mathrm{PL}}$ where $\hbar\omega_{\mathrm{exc}}$ denotes the excitation photon energy and $\hbar\omega_{\mathrm{PL}}$ the PL photon energy. In this representation, we clearly see that the PLE intensity exhibits up to 15 oscillations when ΔE is varied. Their maxima occur at fixed spectral positions ΔE. However, one remarks that the envelope of the PLE onto which these modulations due to phonons are superimposed shows an absolute maximum. Comparing the different PLE spectra in Fig. 5, one remarks that this absolute maximum shifts to higher ΔE for decreasing $\hbar\omega_{\mathrm{PL}}$ values. This supports the assumption that the local maximum in the absorption spectrum corresponds to QD absorption, a point that will be expanded upon later. The PLE intensity modulation with varying ΔE indicates that the photogenerated electron-hole pairs relax by emission of a cascade of phonons of well-defined energies. When the temperature is increased, as we probed up to 100 K, this situation changes and the intensity modulation vanishes for temperatures above 60 K. We therefore conclude that additional scattering with acoustical phonons becomes efficient at this temperature before recombination of the *e-h* pairs occurs.

IV. PHONON ENERGIES

A. Phonon cascade in the QW

We first analyze the modulations observed in the PLE spectra at 5.7 K. Let us denote $\hbar\omega_{\mathrm{PL}}$ as the PL photon energy (detection energy) and $E(i)$ $(i=1, 2, 3, ...,$ etc.) as the energetic position of the ith maxima (from the PL position $\hbar\omega_{\mathrm{PL}}$) observed in a PLE spectrum. The energy separation between a PLE maximum $E(i)$ and the PL spectral position $\hbar\omega_{\mathrm{PL}}$ corresponds to an integer number of the LO phonon energy. For a given PL emission energy, two neighboring PLE maxima are thus related to cascades whose phonon number differ by 1. Figure 6 shows the cascade process schematically. We label Δ_1 the energy separation between the spectral position of the QD PL emission and the first PLE intensity maximum $[\Delta_1 = E(1) - \hbar\omega_{\mathrm{PL}}]$, Δ_2 that between the first and the second PLE maxima $[\Delta_2 = E(2) - E(1)]$, and so on. Then, $\Delta_i = E(i) - E(i-1)$ is the energy of the first phonon in the cascade process involving i phonons. Figure 7 shows the phonon energy Δ_i as a function of the number of phonons i involved in the relaxation process. One clearly sees that the energy of the phonons is not constant but depends on i. At this point it is important to notice that the QW's and QD's consist of ternary CdZnTe with different Cd and Zn concentrations, while only the barriers are made of pure ZnTe. The LO phonon energy for pure ZnTe and pure CdTe is known to be 25.8 and 21.1 meV, respectively. These values have been determined in bulk material by Raman scattering at low tem-

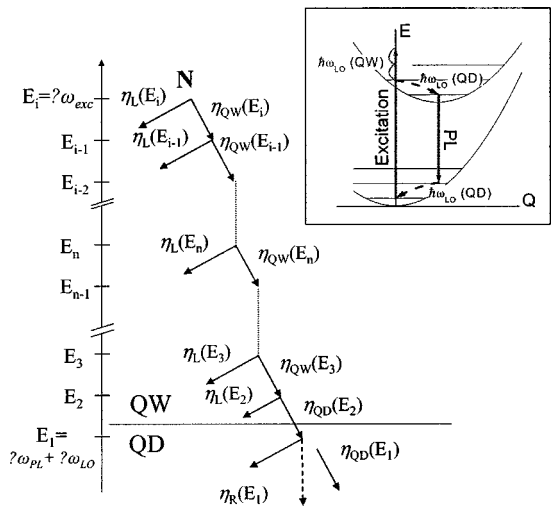

FIG. 6. Scheme of the phonon emission cascade. The inset shows our model involving configuration coordinates for the cascade $i=4$.

peratures in Ref. 13. In a $Cd_xZn_{1-x}Te$ alloy, the LO phonon energy depends on the Cd concentration x and lies between these two values. Let us suppose that we can neglect quantum confinement of phonons and that the bulk values remain valid in the QW's. From Fig. 7, we conclude that bulk ZnTe phonons are emitted only for $i=12$ (and perhaps higher). As determined from the cascades $i=3-11$, the energies of the first emitted phonons in the relaxation processes correspond to Cd concentrations from $x=0.4-0.2$. These are typical values for the matrix in which the QD's are embedded.[12] We therefore conclude that the relaxation processes take place under emission of phonons of the Zn-rich QW's.

B. Trapping in the QD's

Thus only the first and perhaps second phonons ($i=1$ and 2) correspond to a relaxation involving a phonon of the QD material. The QD's are Cd rich, and from the phonon energy Δ_1 we determine $x=0.8$. This value is in good agreement with results obtained by the analysis of HRTEM (Ref. 12)

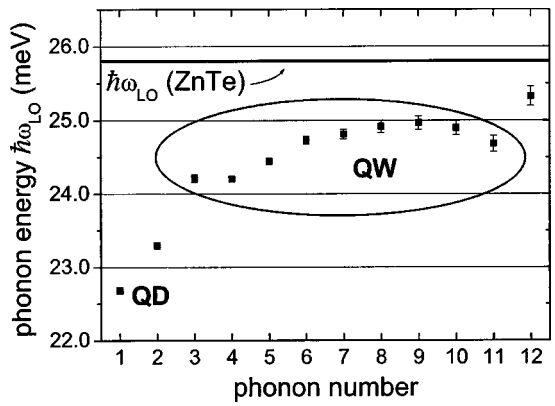

FIG. 7. Phonon energies Δ_i involved in the cascade process as function of the order of emitted phonons *i*. The phonon energies Δ_i are determined from the PLE modulation of Fig. 2.

measurements of the QD's. At low temperatures, after relaxation with emission of QW phonons, the electron-hole pair is trapped in localized QD states and recombines radiatively without further thermalization. Such QD states are always available because of the large inhomogeneous broadening of the luminescence band due to radius, shape, and concentration fluctuations in the dots.

As discussed above, we suppose that the maximum observed in the absorption spectrum (Fig. 1) is due to the QD's. This assumption is supported by the observation of a similar maximum in the envelope of the PLE spectra of Fig. 5. For PL photon energies smaller than that of the luminescence maximum, the PLE envelope shows a maximum located at two phonon energies from the PL emission, while there is no maximum (apart from the modulation due to the phonons) for emissions at higher photon energies. Let $\hbar\omega_{LO}$ denote the energy of the optical phonon. From the Stokes shift $\Delta_{AL}=\hbar\omega_A^M-\hbar\omega_{PL}^M=44$ meV between the luminescence and absorption maxima, we obtain the Huang-Rhys factor $S=\Delta_{AL}/2\hbar\omega_{LO}$ which gives the mean number of phonons involved in the electronic transition of a QD. Using in our case the phonon energy of the QD $\hbar\omega_{LO}=\Delta_1$ we find a Huang-Rhys factor $S=\Delta_{AL}/2\Delta_1=0.96$.

We therefore believe that the observed trapping process is analogous to the mechanism of self-trapped polarons in crystals.[14] As has been discussed in Ref. 15, such electron-phonon bound states may also exist in polar QD's. Surface states inducing a polarization of QD's, for example, have been used to explain the intense PL of Si QD's.[16,17] Using the configuration coordinates Q, an electron-phonon bound state is described by a state of an harmonic oscillator. As indicated in the inset of Fig. 6, the minimum of the potential energy of the QD excited state (i.e., QD with an electron-hole pair) is shifted with respect to that of the ground state (QD with no electron-hole pair). According to the Franck-Condon principle, electronic transitions are vertical, indicating that the lattice deformation cannot instantaneously follow the change of the electronic charge distribution. As a consequence, absorption and emission of a QD transition are spectrally separated. In the case of photoexcitation of the carrier into a QW state, we propose the following trapping and recombination model (as indicated in the inset of Fig. 6 for the case $i=4$): after excitation, the carriers are delocalized in the QW and the QD lattice is not deformed ($Q=0$). After emission of QW phonons, the carriers are trapped in the QD's and their energy is close to the parabola of the excited state at $Q=0$. By emission of another optical phonon, which should be close to the one of the QD, the carrier is trapped in the minimum of the harmonic oscillator potential of the excited state (corresponding to $Q\neq 0$). From this position, without further relaxation, the electron hole pair recombines radiatively. Then the QD comes back to $Q=0$ in the ground state by emitting a QD phonon which is used to restore the lattice deformation. Interpreting the Huang-Rhys factor within this model, a factor of 1 indicates that the crystal deformation energy of the excited state with respect to the ground state is equal to the energy of one optical phonon of the dot. Our experimental results are consistent with this model since the energy Δ_1 corresponds to that of an optical phonon of a QD.

This value is determined with a precision of ± 0.5 meV. At 5.7 K, the energy Δ_2 is neither that of a phonon of the QD nor of the QW, but in between. However, Δ_2 is determined with an error bar of ± 1.0 meV only while all the other Δ_i have errors bar of ± 0.3 meV. At higher temperatures the first two energies (Δ_1 and Δ_2) are that of optical phonons of a QD.

V. QUANTUM EFFICIENCY OF THE PHONON EMISSION

In a simple cascade process indicated in Fig. 6, for $i \geqslant 3$, the ratio of successive emission maxima gives directly the quantum efficiency of the emission of a phonon of the QW. Let us try to explain our results using the following model: We first consider $i \geqslant 3$ and assume that, independently of the photon energy $\hbar\omega_{\mathrm{exc}}$, the exciting light source creates the same number N of electron-hole pairs in the QW layer. After emission of optical phonons, the electron-hole pairs have a random distribution in momentum space whose influence is neglected. We denote by $\eta_{\mathrm{QW}}(E)$ the quantum efficiency that the pair emits a phonon of the quantum well and by $\eta_L(E)$ the probability that the pair is lost for the cascade process. This may be due to radiative recombination, nonradiative recombination processes, trapping on interface states, etc. As we will see, outside the region of QD luminescence, η_{QW} and η_L are almost constant and independent of energy. They fulfill the relation

$$\eta_{\mathrm{QW}} + \eta_L = 1.$$

Inside the QD luminescence region, η_{QW} is replaced by the function η_{QD} and the situation is more complex since $\eta_{\mathrm{QD}}(E_n)$ and $\eta_L(E_n)$ may vary with energy.

Let us assume that the cascade with index i, first, involves $(i\text{-}2)$ emission processes of QW phonons and then one phonon of the QD with the quantum efficiency $\eta_{\mathrm{QD}}(E_2)$. The radiative recombination of the electron-hole pairs occurs with a quantum efficiency $\eta_R(\hbar\omega_{\mathrm{PL}})$, followed by another phonon emission in the dot $\eta_{\mathrm{QD}}(E_1)$. Both $\eta_{\mathrm{QD}}(E_n)$ and $\eta_R(\hbar\omega_{\mathrm{PL}}=E_0)$ may depend on energy. As stated above, this is certainly the case for $\eta_{\mathrm{QD}}(E_n)$. The PLE intensity of the order i cascade is then given by

$$I^i(\hbar\omega_{\mathrm{PL}}) = N\left\{\prod_{n=2}^{(i)} [n_{\mathrm{QW}}(E_n)]\right\} \eta_{\mathrm{QD}}(E_2)\,\eta_R(E_1),$$

where $I^i(\hbar\omega_{\mathrm{PL}}) = I(\hbar\omega_{\mathrm{exc}}=E_i, \hbar\omega_{\mathrm{PL}})$ is the emission intensity at the photon energy $\hbar\omega_{\mathrm{PL}}$ for an excitation at $\hbar\omega_{\mathrm{exc}} = E_i$.

The same QD's, emitting at $\hbar\omega_{\mathrm{PL}}$, can be reached by another phonon cascade, namely one involving one less phonon and starting at a lower excitation photon energy. The PLE intensity of the order $i-1$ cascade for the same value of $\hbar\omega_{\mathrm{PL}}$ is given by

$$I^{i-1}(\hbar\omega_{\mathrm{PL}}) = N\left\{\prod_{n=2}^{(i-1)} [\eta_{\mathrm{QW}}(E_n)]\right\} \eta_{\mathrm{QD}}(E_2)\,\eta_R(E_1),$$

where $I^{i-1}(\hbar\omega_{\mathrm{PL}}) = I(\hbar\omega_{\mathrm{exc}}=E_{i-1}, \hbar\omega_{\mathrm{PL}})$. This means that if two cascades end in the same quantum dot emitting at the energy $\hbar\omega_{\mathrm{PL}}$, the ratio between the emitted luminescence intensities gives the quantum efficiency of the supplementary phonon emission. This efficiency can thus be calculated from the ratio of successive PLE maxima:

$$I^{(i)}(\hbar\omega_{\mathrm{PL}})/I^{(i-1)}(\hbar\omega_{\mathrm{PL}}) = \eta_{\mathrm{QW}}(E_i) = \eta_{\mathrm{QW}}^{(i)}.$$

Formally, the considerations given above hold also for $i=2$, but the model breaks down when the QD's are directly excited for $i=1$ and $i=2$.

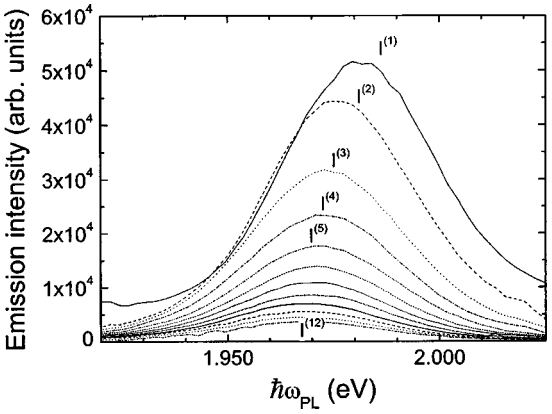

FIG. 8. Intensity of emission phonon energy following the i-phonon line. This corresponds to cross sections of Fig. 2 along lines which are parallel to the diagonal.

Figure 8 shows the intensities $I^i(\hbar\omega_{\mathrm{PL}})$ as a function of the emission photon energy $\hbar\omega_{\mathrm{PL}}$. Each curve $I^i(\hbar\omega_{\mathrm{PL}})$, which represents the PL spectrum when dots are selectively populated with an i-phonons cascade, is obtained from the data of Fig. 2 by taking the value of the PL intensity maximum (corresponding to a given phonon number i) along a line parallel to the diagonal. As the phonon energy can vary as a function of E_n depending on the cadmium concentration, we obtain

$$\hbar\omega_{\mathrm{exc}} = E_i = \sum_{n=1}^{i} \hbar\omega_{\mathrm{LO}}(E_n) + \hbar\omega_{\mathrm{PL}} \approx i\hbar\omega_{\mathrm{LO}} + \hbar\omega_{\mathrm{PL}}.$$

The quantum efficiency can change along such a line of maxima, i.e., vary as a function of E_i. Figure 9 shows

$$\eta_{\mathrm{QW}}^{(i)} = \eta_{\mathrm{QW}}(E_i) = I^{(i)}(\hbar\omega_{\mathrm{PL}})/I^{(i-1)}(\hbar\omega_{\mathrm{PL}})$$
$$= I(\hbar\omega_{\mathrm{exc}}=E_i, \hbar\omega_{\mathrm{PL}})/I(\hbar\omega_{\mathrm{exc}}=E_{i-1}, \hbar\omega_{\mathrm{PL}})$$

for the cascades $i=3-12$ as functions of the excitation photon energy E_i. The regions plotted in Fig. 9 by dots correspond to the observed PL band between 1.950 and 2.000 eV which can be analyzed for all cascades: for each phonon index i in Fig. 9, data points for low-excitation photon energies E_i correspond, for example, to low PL emission photon energies $\hbar\omega_{\mathrm{PL}}$. For $i \leqslant 7$ a larger spectral region can be analyzed and the results are indicated by full lines.

A. Phonon cascade in the QW

As discussed above, the emission photon energy $\hbar.\omega_{\mathrm{PL}}$ is strictly determined by the cascade index i and excitation pho-

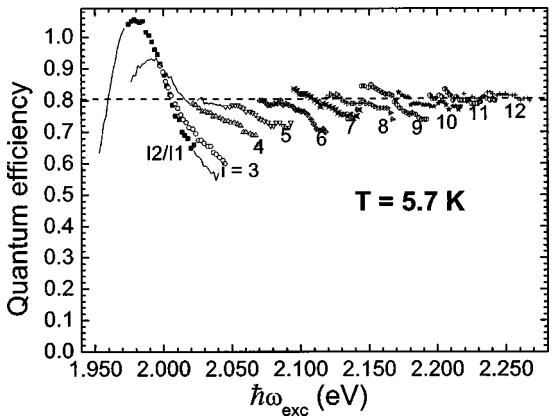

FIG. 9. Quantum efficiency $\eta_{QW}^{(i)}=I^{(i)}/I^{(i-1)}$ determined from Fig. 2 as function of photon energy of excitation $\hbar\omega_{exc}$ for different orders of emitted phonons $i\geqslant 3$. Quantum efficiencies $\eta_{QW}^{(i)}$ giving rise to PL between 1.950 and 2.000 eV can be determined for all cascade indices *i*. In this region the results are given by dots. For $i<8$ and small PL photon energies, a larger spectral region can be analyzed. Full lines indicate the results. In addition, the intensity ratio $I^{(2)}/I^{(1)}$ is given.

ton energy E_i. Thus the $\eta_{QW}^{(i)}$ data can be analyzed as a function of both E_i or $\hbar\omega_{PL}$. For $i>9$, $\eta_{QW}^{(i)}$ is constant with respect to the exciting photon energy E_i, the cascade index *i*, and, consequently, to the PL photon energy. When the PL is detected at low photon energies, around 1.950 eV, the quantum efficiency of the phonon emission is very high, around 0.8, and is independent of the cascade index *i*. It corresponds to the emission of QD's with a large radius. For a given index $i\leqslant 9$, $\eta_{QW}^{(i)}$ decreases linearly with increasing PL or excitation energies (corresponding to dots of smaller radius). In addition, the slope of $\eta_{QW}^{(i)}$ also depends slightly on the cascade index *i* for $4\leqslant i\leqslant 9$.

Since for a given photon energy $\hbar\omega_{PL}$ of luminescence the same QD states are involved in the emission process, independent of the index *i* of the cascades, a variation of $\eta_{QW}^{(i)}$ with *i* has to be attributed to the properties of the electron-hole pairs which become trapped. We tentatively attribute the PL energy and cascade index *i* dependence of $\eta_{QW}^{(i)}$ to the fact that initially, all electron-hole pairs are created in the QW with a center-of-mass wave vector $K=0$. By emission of optical phonons the distribution of wave vector becomes more and more random when the order of the cascade increases. In the smaller QD's, the electronic wave functions are more localized than in the larger ones. These wave functions spread more in *K* space for the smaller QD's. Consequently, the transition of delocalized QW excitons from a distribution well peaked around $K=0$ towards localized states in the QD's will be privileged for the larger QD's. If this interpretation is correct, it means that, if $i\geqslant 9$, the distribution is fully randomized and does not change with *i*, i.e., with the size of the QD. For smaller cascade index, the electron-hole pair distribution remains peaked at $K=0$ and large QD's are populated more easily. Another reason for this result could be that the number of photoexcited electron-hole pairs is not really the same when comparing different cascades since the absorption of the sample depends on the photon energy of excitation. We can, however, exclude this possibility because the quantum efficiency $\eta_{QW}^{(i)}$ for emitting photons at 1.950 eV is almost constant when varying the photon energy of excitation between 2.020 and 2.300 eV.

B. Trapping in the QD's

For $i=2-4$, we do no longer observe the slight linear dependence of $\eta^{(i)}$ on the PL energy at low photon energies. For these cascades, the intensity ratios show a well defined maximum at 1.971 eV, i.e., at the position of the luminescence maximum.

One possibility is that, while under nonresonant excitation conditions, the recorded intensity is due to pure PL, when exciting close to or inside the PL band, the recorded signal should additionally be enhanced due to resonant Raman scattering, a process not considered in our model.

This hypothesis is not essential, however, as our model can describe these results obtained under resonant excitation conditions. As explained above, we believe that the trapping mechanism itself involves the interaction with optical phonons of the QD's (inset of Fig. 6). The crystal deformation leads to the creation of a self-trapped state of lower energy. From this state, the electron-hole pair recombines with emission of an optical phonon. Its energy is used to restore the lattice deformation. Transitions between the excited and ground QD states can involve any number of phonons but their respective probabilities depend strongly on the equilibrium position displacement between the excited and ground state. The Huang-Rhys factor determines them and gives the mean number of phonons involved in both excited- and ground-states relaxation. This model is thus supported by our experimental results obtained under resonant excitation conditions: A value of the Huang-Rhys factor close to 1 leads to a two-phonon line which is more intense than the one-phonon line. This explains that the ratio $I^{(2)}/I^{(1)}$ (Fig. 9) is greater than unity and shows that the mean number of phonons involved in both the excited and ground state relaxation is 1. This is a further indication of the important coupling between electronic and vibrational modes in the CdTe QD's.

C. Temperature dependence

When increasing the temperature from 5.7 to 100 K the results given in Fig. 9 remain quantitatively the same, at least within the error bars. This indicates that the quantum efficiency of optical-phonon emission is independent of temperature in this range. As stated above, the modulation of the PLE intensity diminishes and vanishes above $T=60$ K since thermalization with acoustical phonons becomes possible. The state of self-trapped polarons is no longer stable. Concerning the phonon energies involved in the cascades, the only difference observed with respect to Fig. 7 is that for $T\geqslant 30$ K the energy of the $i=2$ phonon is the same as that of $i=1$. This implies that phonons of the quantum dots are emitted in both relaxation processes.

VI. CONCLUSIONS

We have determined the relaxation scenario of an electron-hole population after excitation of the Zn-rich CdZnTe quantum wells in which Cd-rich quantum dots are embedded. We have shown that the energy relaxation is characterized by emission of cascades of longitudinal optical phonons in the quantum well. The quantum efficiency of this process is very high (about 0.8) and almost independent of energy and temperature. The small energy dependence of the quantum efficiency, which is mainly observed when only a small number of phonons are implied in the relaxation cascade, is tentatively attributed to the fact that the center-of-mass wave vector of the electron-hole distribution in the QW becomes more and more random as the phonon cascade proceeds.

During these relaxation processes, the electron-hole pairs do not recombine radiatively. When the electron-hole pairs have an energy just in excess of the lowest quantum dot level, they emit a phonon and become trapped without further energy relaxation. This trapping is then followed by a radiative recombination. Since the maxima of absorption and emission of the QD's are separated by about two times the energy of the optical phonon of the QD's, we believe that the trapping mechanism itself involves the interaction with optical phonons of the QD's. The lattice deformation leads to the creation of a self-trapped state of lower energy. This also explains why further energy relaxation with emission of acoustical phonons is not observed at low temperatures since the self-trapped state is the lowest excited state of the quantum dot having trapped an electron or a hole. From this state, the electron-hole pair recombines with emission of an optical phonon to restore the lattice deformation. Under resonant excitation conditions, the observed PL reflects the original emission line shape of *e-h* pairs when coupled to vibrationnal modes of the QD's.

With increasing temperature the lattice polarization disappears, and the state of self-trapped polarons is no longer stable. Then, the PLE modulation washes out since thermalization with acoustical phonons becomes possible.

*Corresponding author. Email address: Pierre.Gilliot@ipcms.u-strasbg.fr

[1] H.-P. Tranitz, H. P. Wagner, R. Engelhardt, U. W. Pohl, and D. Bimberg, Phys. Rev. B **65**, 035325 (2002).
[2] F. Gindele, U. Woggon, W. Langbein, J. M. Hvam, K. Leonardi, D. Hommel, and H. Selke, Phys. Rev. B **60**, 8773 (1999).
[3] H. P. Wagner, H.-P. Tranitz, H. Preis, W. Langbein, K. Leosson, and J. M. Hvam, Phys. Rev. B **60**, 10 640 (1999).
[4] H. P. Wagner, H.-P. Tranitz, H. Preis, W. Langbein, and J. M. Hvam, J. Cryst. Growth **214/215**, 747 (2000).
[5] H. P. Wagner, H.-P. Tranitz, R. Schuster, R. Engelhardt, U. W. Pohl, and D. Bimberg, Phys. Status Solidi B **224**, 195 (2001).
[6] U. Woggon, F. Gindele, W. Langbein, and J. M. Hvam, Phys. Rev. B **61**, 1935 (2000).
[7] N. H. Bonadeo, Gang Chen, D. Gammon, and D. G. Steel, Phys. Status Solidi B **221**, 5 (2000).
[8] Y. Viale, P. Gilliot, O. Crégut, J.-P. Likforman, B. Hönerlage, R. Levy, L. Besombes, L. Marshal, K. Kheng, and H. Mariette, Mater. Sci. Eng., B **101**, 55 (2003).
[9] R. Heitz, M. Veit, N. N. Ledentsov, A. Hoffmann, D. Bimberg, V. M. Ustinov, P. S. Kop'ev, and Zh. I. Alferov, Phys. Rev. B **56**, 10 435 (1997).
[10] Y. Masumoto, M. Nomura, T. Okuno, Y. Terai, S. Kuroda, and K. Takita, J. Lumin. **102**, 623 (2003).
[11] L. Marsal, L. Besombes, F. Tinjod, K. Kheng, A. Wasiela, B. Gilles, J.-L. Rouvière, and H. Mariette, J. Appl. Phys. **91**, 4936 (2002).
[12] L. Besombes, Ph.D. thesis, Université Joseph Fourier, Grenoble, France, 2001.
[13] D. J. Olego, P. M. Raccah, and J. P. Faurie, Phys. Rev. B **33**, 3819 (1986).
[14] Y. Toyozawa and J. Hermanson, Phys. Rev. Lett. **21**, 1637 (1968).
[15] T. Stauber, R. Zimmermann, and H. Castella, Phys. Rev. B **62**, 7336 (2000).
[16] G. Allan, C. Delerue, and M. Lannoo, Phys. Rev. Lett. **76**, 2961 (1996).
[17] M. H. Nayfeh, N. Bary, J. Therrien, O. Akcakir, E. Gratton, and G. Belomoin, Appl. Phys. Lett. **78**, 1131 (2001).